[1, *]**Sushil Kumar Bhoi**

[1]**Pradeep Kumar Shill**

[1]**Niranjan Behera**

[1]**Asini Kumar Baliarsingh**

[2]**Dilip Kumar Bagal**

Voltage Control of PV-Wind-FC-Electrolyzer-Battery based Hybrid Microgrid

JES

Journal of Electrical Systems

Abstract: - The global community is actively exploring methods to utilize renewable energy sources (RESs) to address global warming and decrease dependence on fossil fuels. Wind and solar energy have become popular choices in various regions worldwide. On the other hand, wind speed and sun irradiation are determined by nature and cannot be regulated as needed. Therefore, incorporating an energy storage system is crucial to maximize the use of these energy sources by converting them into electricity. Batteries are a standout option among various energy storage choices for medium power applications. Nonetheless, batteries require significant maintenance and are susceptible to self-discharge, resulting in a gradual decrease in storage capacity over time. For high power applications, hydrogen storage emerges as a cost-effective alternative to batteries. Stored hydrogen can be utilized for transportation and electricity generation. An electrolyzer can effectively produce hydrogen and oxygen from water by using electric power. However, slow heat transfer dynamics impede the rapid production of hydrogen, necessitating an innovative control technique to enhance production quality during fluctuations in wind speed and solar irradiances. In order to enhance energy efficiency, it is essential for wind turbines and photovoltaic panels to function at their peak capacities. The Whale Optimization Algorithm (WOA) is incorporated into the control systems of boost converters, which are used in this study as maximum power point tracking mechanisms. This allows for consistent hydrogen production even in the face of sudden variations in wind speed and sunlight intensity. WOA's efficacy is compared to other optimization methods, including PSO (particle swarm optimization), GA (genetic algorithm), and GWO (grey wolf optimization), in order to demonstrate the benefits of real-time system monitoring for augmenting hydrogen production from a mix of RESs in a microgrid. This research proposes a unique control strategy to stabilize voltage under a range of operating situations. MATLAB is used to display the findings of the investigation.

Keywords: Battery, Electrolyzer, Fuel Cell (FC), Microgrid, Photovoltaic (PV), Whale optimization, Wind.

I. INTRODUCTION

Providing electricity to consumers in regions without utility grids remains a challenging endeavor. However, a viable solution to address this issue is the establishment of localized small-scale independent microgrids. These microgrids utilize RESs, making them environmentally friendly. By integrating various RESs such as solar power through Photovoltaic (PV) technology and wind energy through PMSG: Permanent Magnet Synchronous Generator technology, these systems can be reliably to delivering high-quality electricity to consumers residing in remote areas.

Solar irradiance and wind velocity are two variables that are constantly changing, causing fluctuations in power generation. In order to maintain a stable balanced power in a standalone microgrid, it is crucial to make use of an energy storage device. While batteries are a popular choice for energy storage, they may not be sufficient for high-power applications over long periods of time. Additionally, battery has a limited lifespan and requires daily maintenance and replacements, leading to high costs. A compact battery storage system (BSS) and an electrolyzer system (ES) combined with a fuel cell (FC) are included into the system to solve these issues. While the FC-ES combination runs slowly to maintain power balance during stable states, the BSS may react swiftly to abrupt changes in the environment. When generation exceeds demand, the FC-ES set uses electrolysis to create hydrogen from water. This hydrogen is then stored in a tank and used by the FC to generate electricity to meet demand. The microgrid becomes more economical by using hydrogen for long-term storage and batteries for short-term power

---

[1] *Corresponding author: Department of Electrical Engineering, Government College of Engineering Kalahandi, Bhawanipatna, Kalahandi, Odisha, India, PIN-766003 (sushilkumarbhoi@gmail.com, pkshill92@gmail.com, niranjan.265@gmail.com, and asinikumar333@gmail.com)

[2] Department of Mechanical Engineering, Government College of Engineering Kalahandi, Bhawanipatna, Kalahandi, Odisha, India, PIN-766003 (dilipbagal90@gmail.com)

supply. However, effective energy management is essential to supply quality power to loads in microgrids. Hence, an optimization method can be implemented to efficiently manage energy and enhance hydrogen production through informed decision-making. Among various optimization methods, the WOA is notable for its ability to determine the optimal decision for maximizing output production despite random fluctuations in inputs such as irradiance, wind speed, and load. In light of these limitations, this study presents an energy management system (EMS) based on WOA, whose goal is to minimize the microgrid's overall cost function while boosting hydrogen generation. Additionally, the report details the implementation of an inverter control system that is specifically developed to maintain a consistent voltage at the load bus, even when faced with unbalanced voltage scenarios, ultimately enhancing the quality of power.

II. STANDALONE PROPOSED SYSTEM

The standalone microgrid, which is based on RESs, is depicted in Figure 1.
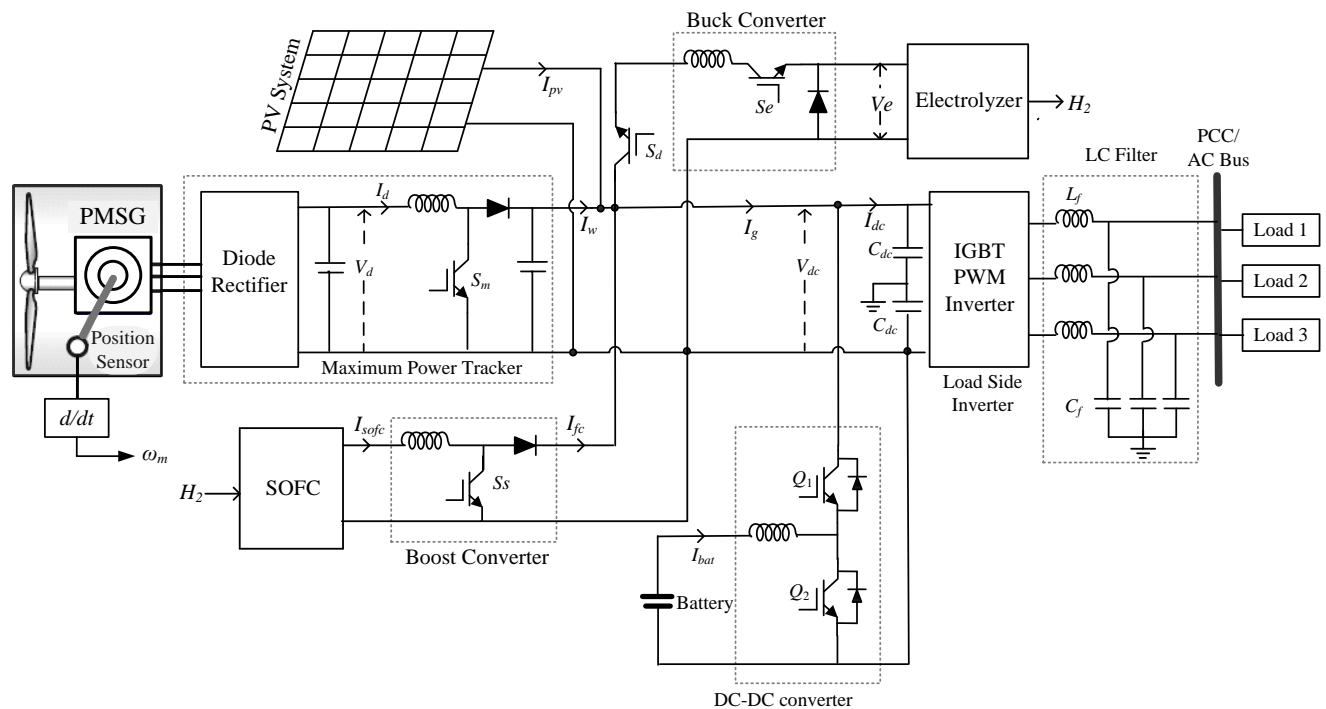
Figure 1: Microgrid power supply model.

Previous studies have extensively analyzed the hybrid microgrid, which shares similar standalone features [8-14]. The power management strategy proposed by the authors aimed to regulate the different components within the microgrid [8]. In [9], the authors showcased the utilization of RESs for hydrogen production. However, [10] implemented a greenhouse powered by RESs, but it was specifically designed for single-phase applications. The study conducted by the authors in reference [11] showcased the production of hydrogen using RESs, however, they failed to discuss the concerns related to power quality. Reference [12] shown a DC microgrid designed for hydrogen production utilizing RESs. Additionally, reference [13] formulated an energy management method for a standalone system, yet they overlooked unbalanced issues and power quality issues. In reference [14], a comparative analysis was carried out on various EMSs for wind, hydrogen and PV operated Microgrid. It is crucial to highlight that the authors referenced in [8-14] did not integrate optimization mechanisms to increase hydrogen production.

The document details the creation of a microgrid that makes use of RESs, aiming to achieve the following goals:

a)   Effective control coordination has been implemented for wind, PV, FC, battery, and electrolyzer systems.

b)   Effective regulators have been employed to maintain the voltage at the load terminal, despite changes in wind or PV power generation and load fluctuations.

c)   Maintaining balanced voltages is essential to guarantee stable voltage levels at the load bus when unbalanced currents are present in a three-phase system.

d)   Create a highly effective energy management system that utilizes the WOA mechanism to enhance hydrogen production and ensure consistent power quality in any situation.

The BSS, DC-ink, and bidirectional DC to DC buck-boost circuit are integrated. As shown in Figure 2, the DC-DC converter control regulates the BSS charging and discharging procedure to keep the voltage steady. The BSS's current reference is established by the controller's output. To provide the required switching signals for switches Q_1 & Q_2 of the converter, a hysteresis loop is set up. As shown in Figure 2, the converter's controller incorporates the State of Charge (SoC) to avoid overcharging or discharging of the BSS.

When the BSS's SoC hits its upper limit, the excess power will be used by the ES to create oxygen and hydrogen. In a similar vein, at steady state, the FC will provide enough power to fulfill load demands when the SoC reaches the minimum set point. Because of its dynamics, the FC cannot provide power instantly, which causes a voltage fall at the DC-link under temporary circumstances. To ensure stability of the voltage regardless of any variations in the system, it is crucial to implement proper control coordination among all components in a microgrid. Figure 3 and Figure 4 illustrate the appropriate control mechanisms for the buck converter (used for the ES) and the boost converter (used for the FC), respectively. The designed controllers for all dc to dc circuits are configured in a way that the BSS responds immediately to sudden load changes, while the ES-FC set operates steadily. When the SoC hits 20.0% and switch Q_2 of the DC-DC circuit is turned on (while Q_1 is turned off), the FC begins generating the required electricity, with the battery maintaining its state V_{dc}^*. Figure 5 shows how the microgrid's energy management is shown. The control method for increasing a wind turbine's power generating efficiency is taken from [1]. In order to do maximum power point tracking (MPPT) without the need for a separate converter, the PV unit is linked to the DC-bus directly. The buck converter of the ES and the DC to DC bidirectional circuit, which serve as the MPPT circuit for the PV system, are integrated with the PV's MPPT algorithm. Multiple single-phase loads linked in a distribution power system will cause imbalanced currents in the three-phase system. The second oscillating harmonic component will be present in the DC-link voltage when unbalanced loads are operating. The fatigue life of the shaft may be impacted by vibrations brought on by this second harmonic component. An active filter [15] on the dc-side is also combined with the control techniques of the DC to DC circuits connected to BES, ES, and FC in order to lessen the consequences of this effect. The dc component (V_{dc}') will be extracted through low pass filter from V_{dc} and the oscillating component (V_{dco}) got by subtracting V_{dc}' from V_{dc}. To remove the voltage oscillations, the value of '0' acts as a reference signal for the second PI. Combining the outputs of both PIs yields the final reference current.
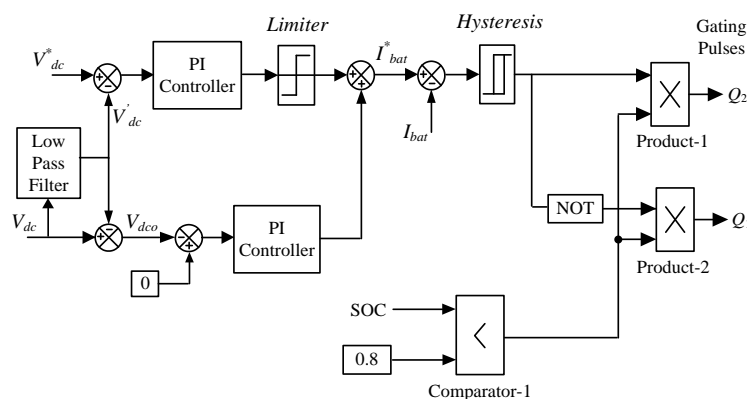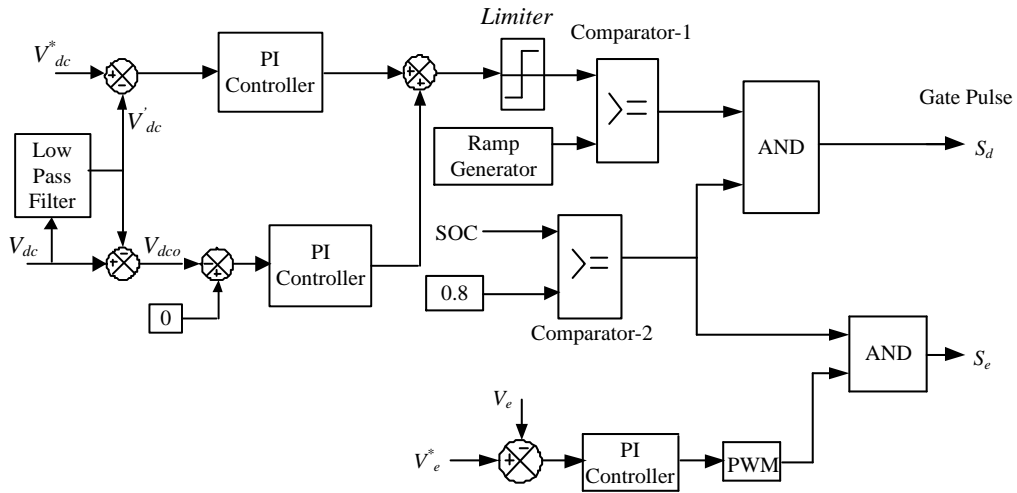

Figure 2: Control mechanism of bidirectional converter.
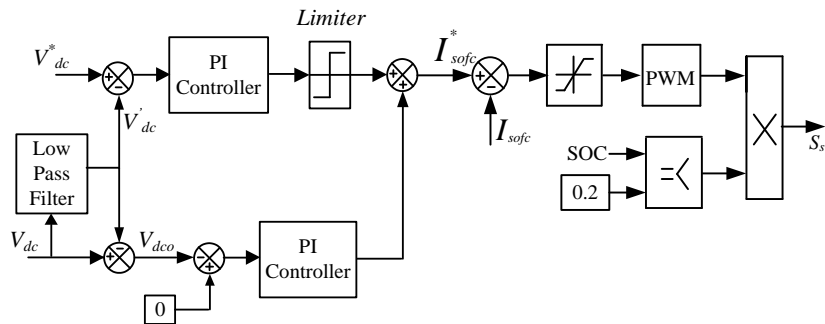
Figure 3: Control method for buck converter.

Figure 4: Control mechanism of boost converter.

Unbalanced voltages across the three phases occur when there is an unbalanced load at the PCC: point of common coupling. This imbalance is caused by unequal drops across the 'LC' filter in each phase. In order to address this problem, a dedicated inverter controller has been developed. This controller generates unique modulation indexes for every phase, ensuring balanced voltages at PCC. The implementation of the proposed control method of inverter based on dq0 is depicted in Figure 6.
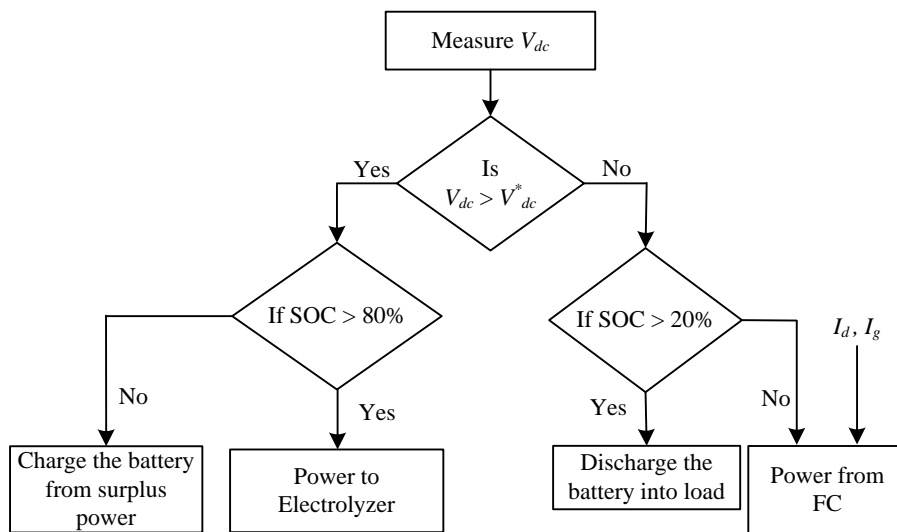
Figure 5: Energy management algorithm.
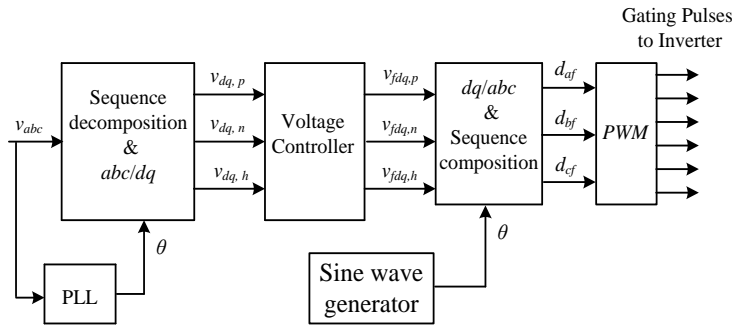
Figure 6: dq0 based proposed inverter controller.

III. APPLICATIONS OF WOA

Determining the appropriate unit sizing is a critical aspect in a standalone model, especially one that relies on RESs. This is crucial because it keeps the system's total cost down while guaranteeing loads get a steady and dependable power supply [16–17]. In order to do this, the HOMER program is used to calculate the ideal unit size depending on the load profile [8] (i.e., Figure 7). The model's technical and economic data comes from [8, 18]. By utilizing the HOMER software, the optimal sizes for the wind and PV components are determined to be 15kW and 20.4kW respectively. As a result, this study considers the utilization of two PV arrays, each with a capacity of 7.50kW, and three wind turbines, each with a capacity of 6.8kW.
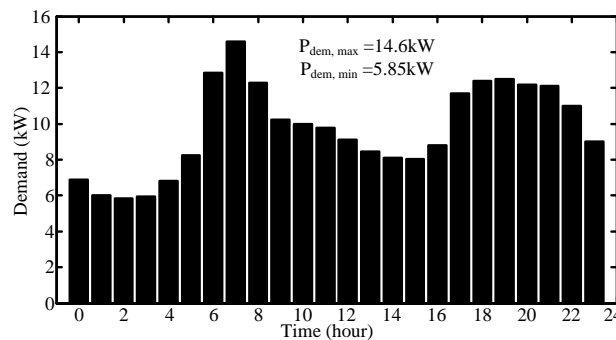
Figure 7: Load values [8].

The FC is expected to manage the peak load without relying on power from RESs. As a result, the FC's required rating in this study is 18kW, with an additional 20% rating for optimal performance. Similarly, the electrolyzer's rating is determined based on the surplus power available. Taking into account 60.0% of the maximum surplus power from RESs, the ES rating is calculated as follows:

Electrolyzer size = (Total production in Kw – Minimum load in Kw) $\times$ 0.60.

$$=(15.0+20.40-5.85) \times 0.60 = 17.73 \text{kW}.$$

Nevertheless, the expressed cost function encompasses the expenses associated with capital, maintenance, operations, replacements, salvages, electricity purchases, electricity sales, and hydrogen sales.

Cost function = C_{GP}-C_{GS}-C_{HS}+C_{CAP}+C_{OM} +C_{REP}-C_{DTB}-C_{SV} (1)

In this context, CCAP represents the capital cost, COM stands for operation and maintenance cost, CREP denotes replacement cost, CDTB signifies depreciation tax benefit, CSV indicates salvage value, CGP and CGS refer to purchase and selling costs, and CHS represents hydrogen selling price.

Hence, "C" (cost function) is:

$$\sum_{t=1}^{n} C = \left(C_{mg} \times E_{mg} \right) \tag{2}$$

If $E_{mg} < 0$, C_{mg} is the variable electricity price based on hourly data.

As a result, the following equations may be used to get the components' dimensions:

$$E_{D(e)} = E_{mg} + E_{WT} + E_{Hy} + E_{PV} - E_{EL(e)} + E_{FC(e)} \tag{3}$$

$$E_{D(H2)} = E_{EL(e)} \, \eta_{EL}^{e/H2} \pm E_{inj(H2)} - E_{FC(e)} \, \eta_{FC}^{\frac{1}{H2/e}} \tag{4}$$

Where, Where, E_{mg}= Microgrid electricity.

Typically, the amount of hydrogen produced (flow rate) from an ES can be determined using the following equation:

$$Q = 80.7 \times \eta_F \frac{n_c I_{dc}}{ZF} \tag{5}$$

$$\eta_F = \frac{\left(\dfrac{I_{dc}}{A} \right)^2}{f_1 + \left(\dfrac{I_{dc}}{A} \right)^2} f_2$$

Where,

The electrode's surface area is symbolized by 'A', Z stands for the number of electrons, the Faraday constant is represented by 'F'. The variable nc indicates the number of cells, while Idc denotes the current flow within the ES.

The aforementioned equation provides a clear indication that the rate at which hydrogen is produced is directly influenced by the current passing through the electrodes. As a result, a buck converter is required to lower the voltage and then increase the current on the ES side. This modification helps to raise the current, which makes it possible for the system to produce more hydrogen overall. However, it's crucial to remember that the ES needs a minimum voltage in order to operate, which is represented by the following equation:

$$V_{cell} = \frac{\Delta G}{ZF} + s \log \left(\frac{t_1 + \dfrac{t_2}{T} + \dfrac{t_3}{T^2}}{A} I + 1 \right) + \frac{r_1 + r_2 T}{A} I \tag{6}$$

In this context, T represents temperature, ΔG stands for Gibbs Energy, s, t1 to t3 denote overvoltage coefficients on the electrode, and r1, r2 are parameters associated with ohmic resistance.

The buck converter output voltage must be more than V_{cell} to achieve more flow of current in ES.

Hydrogen is produced by the ES and then transported straight into the storage tank. The following equations provide the mathematical representation for the storage tanks:

$$N_{H2} = \frac{N_F N_c}{2F} I_{dc} \tag{7}$$

$$P_b - P_{bt} = Z \frac{N_{H2} R T_b}{M_{H2} V_b} \tag{8}$$

The oxygen and hydrogen can also be utilized to produce electricity again using a Fuel Cell. The equations presented below play a crucial role in the modeling of Fuel Cells [1].

Ideal voltage (E) is:

$$E = E^0 - \frac{RT}{2F} \ln\left(P_{H_2} \times P_{O_2}^{0.5}\right)$$

(9)

$$P_{H2} = 0.5 P_{H2O}^{sat}\left[\exp\left(-\frac{1.635J}{T_{cell}^{1.334}}\right)\left(\frac{P_a}{P_{H2O}^{sat}}\right)-1\right] \quad P_{O2} = P_{H2O}^{sat}\left[\exp\left(-\frac{4.192J}{T_{cell}^{1.334}}\right)\left(\frac{P_c}{P_{H2O}^{sat}}\right)-1\right]$$

Where, , Pc is partial

pressure at cathode, Pa is partial pressure at anode, current density is represented by 'J'.

Voltage due to activation loss is:

$$V_{act} = \beta_1 + T\left[\beta_2 + \beta_3 \ln(CO_2) + \beta_4 \ln(i)\right]$$,

(10)

The voltage drop is

$$V_{ohmi} = -i \times R_{int}$$

(11)

Where $R_{int} = 1.605 \times 10^{-2} - 3.5 \times 10^{-5} T_{cell} + 8 \times 10^{-5} i$

Mass transport losses are the source of concentration losses. The resulting voltage drop may be shown as follows:

$$V_{conc} = B.\ln\left(1 - \frac{i}{i_{lim}}\right)$$

(12)

Where 'B' is a constant and i_{lim} is the limiting current.

Therefore, the following equation will be used to get the fuel cell's voltage:

$$V_{cell} = E - V_{act} - V_{conc} - V_{ohm}$$

(13)
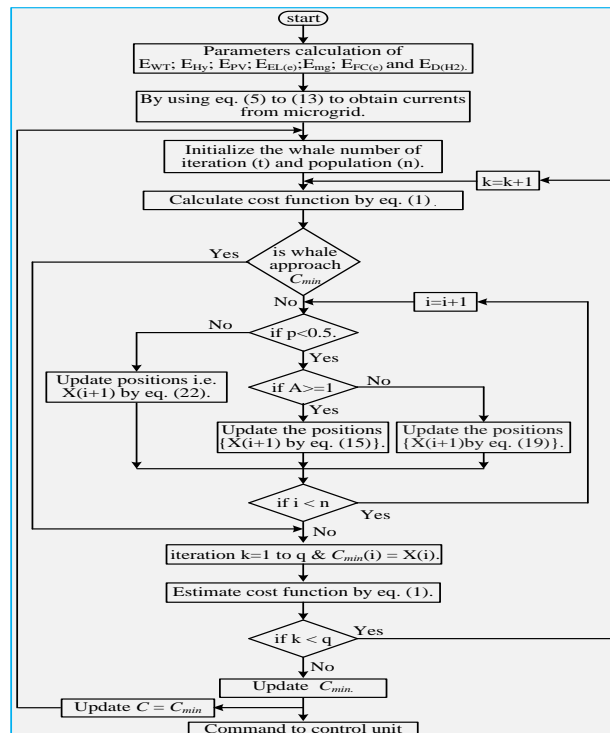
Figure 8: Flow chart for WOA.

A very useful optimization technique for figuring out the least cost function is the WOA. This novel strategy takes its cues from humpback whale hunting techniques. Whales essentially use a bubble net system to snare little fish that are swimming in a circle. The following formulae may be used to quantitatively express this hunting strategy:

$$\vec{D} = \left| \vec{X}(i) - \vec{C} \bullet \vec{X}^{*}(i) \right|$$

(14)

$$\vec{X}(i+1) = -\vec{A} \bullet \vec{D} + \vec{X}^{*}(i)$$

(15)

The location is represented by the position vectors, and the current value of the iteration is indicated by the coefficient 'i'.

The humpback whales are traveling in a decreasing circle in the direction of their prey, as seen by:

$$\vec{D}' = \vec{X}^{*}(i) - \vec{X}(i)$$

(16)

$$\vec{X}(i+1) = \begin{cases} \vec{X}^{*}(i) - \vec{A} \bullet \vec{D} & \text{if } p < 0.5 \\ \vec{X}^{*}(i) + \vec{D}' \bullet e^{bl} \bullet \cos(2\pi l) & \text{if } p \geq 0.5 \end{cases}$$

(17)

$$\vec{D} = \left| \vec{X} - \vec{C} \bullet \vec{X}_{rand} \right|$$

(18)

$$\vec{X}(i+1) = -\vec{A} \bullet \vec{D} + \vec{X}_{rand}$$

(19)

1. The vector   will be reduced by the specified value of   in the shrinking surrounding mechanism.

$$\vec{A} = 2\vec{a} \bullet \vec{r} - \vec{a}$$

(20)

$$\vec{C} = 2 \bullet \vec{r}$$

(21)

The selection of the range assists in determining the updated location of the searching agent, which is chosen from the interval [-a, a].

During this stage, the whale's location will be adjusted based on the proximity of the prey's current position to the closest whales. This mathematical model accurately reflects the spiral movement of the whale.

$$\vec{X}(i+1) = \vec{D}' \bullet e^{bl} \bullet \cos(2\pi l) + \vec{X}^{*}(i)$$

(22)

The microgrid's cost function is optimized using the WOA mechanism to determine the optimal solution for generating the necessary switching pulses for the converter. Figure 8 illustrates the flowchart that identifies the minimum cost function.

IV. RESULTS

To ensure optimal visualization, the results on the MATLAB/Simulink platform are presented using a single wind and PV units. The performance of controllers is evaluated by examining various cases of the microgrid shown in Figure 1.

### A.   Case-1: during unbalanced load operation

The microgrid undergoes testing while taking into account the unbalanced scenario described in Figure 9.

RMS currents of: Phase-1 (ila)= 3.49A;   Phase-2 (ilb) = 9.61A;   Phase-3 (ilc) = 8.51A.

The torque response of the PMSG under imbalanced conditions is shown in Figure 10 with and without the suggested DC to DC circuit technique. Torque pulsations may be lessened using the suggested controller in combination with DC-link voltage management. Nevertheless, the voltages at the PCC will be out of balance as a result of irregular decreases at the filter in each phase. On the other hand, the proposed inverter controller can guarantee that the voltages stay balanced by generating the required modulation indexes (MIs) for every phase. Figure 11 shows the balanced line voltages at the PCC. The RMS values of the phase voltages and the accompanying MIs are shown in Figure 12 for better comprehension.
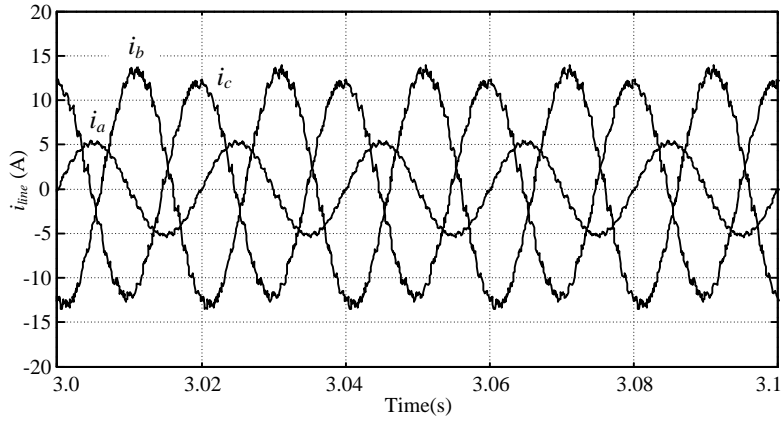
Figure 9: 3-phase currents.
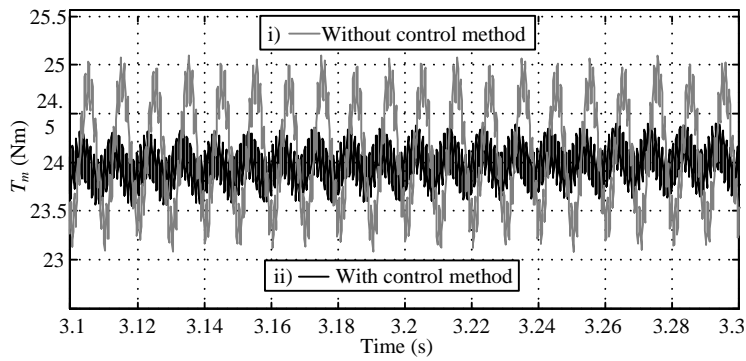
Figure 10: PMSG torques.
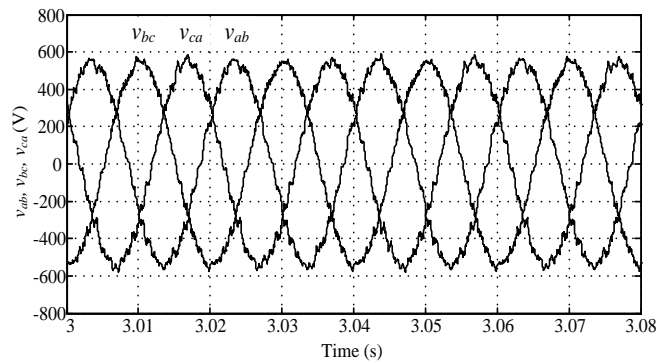
Figure 11: Voltages.
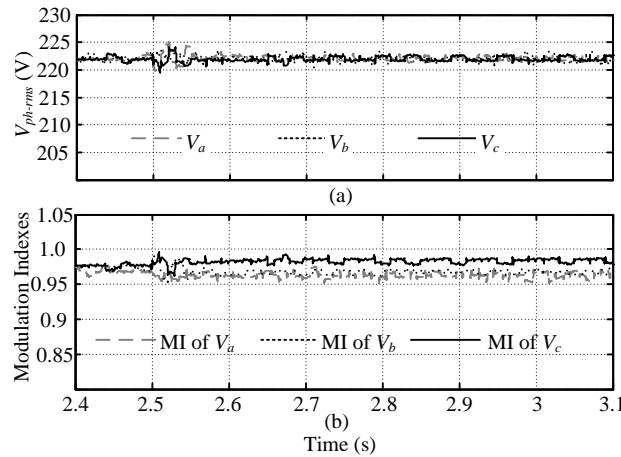
Figure 12: (a) phase RMS voltages; (b) MI.

B.   Case-2: Operation with ES

The ES's functionality is essential to the system's performance. This is accomplished by setting the BSS's SoC to around 80.0% and supposing that more power is available from other sources. According to the EMS described in this article, as Figure 13 illustrates, the ES begins to use the excess power when the BSS's SoC rises over 80.0%. Figure 13 illustrates that the SoC reaches 80.0% at around t=1.95 seconds. Figure 14 shows the response of the voltage at DC-link (via the ES's buck circuit).
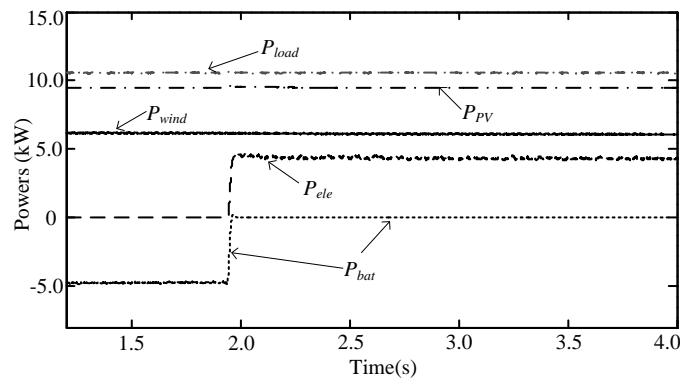
Figure 13: Powers.
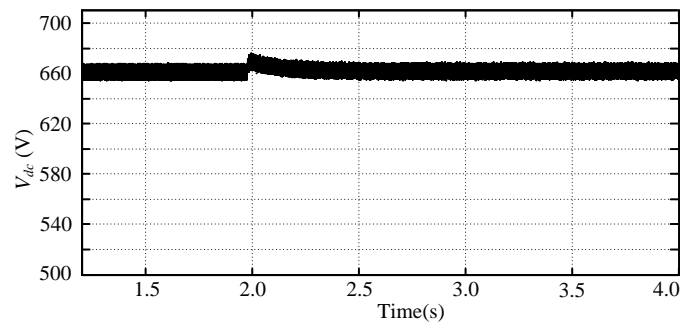
Figure 14: Voltage.

C.   Case-3: Operation with Fuel Cell

By examining the effects of a rapid rise in load from 7.50 to 15.0 kW at t=10.0sec, the microgrid's performance was assessed. In accordance with the suggested EMS, the FC's slower dynamics caused it to provide power gradually, whereas the BES reacted quickly to meet the increasing load requirement. Consequently, at about t=10.95sec, the Battery Storage System's (BSS) State of Charge (SoC) dropped to 20.0% (Figure 15). At t=11.16 seconds, the FC

began delivering power, and it took around t=12.8 seconds to achieve the load requirement. Because of the clever cooperation between the FC and battery, in a steady state the battery power dropped to zero and the FC provided all of the necessary power. This coordination was effectively accomplished by the microgrid's control mechanism, as Figure 16 illustrates.
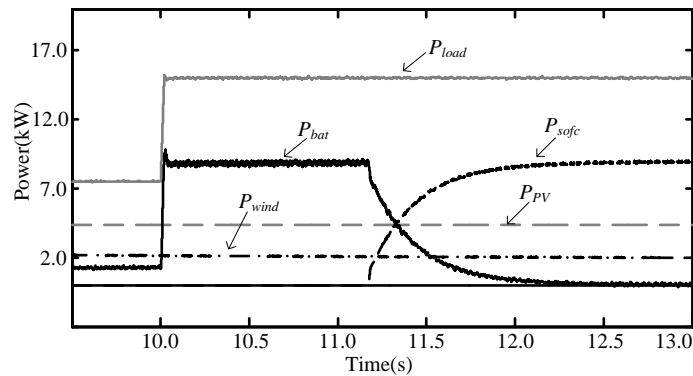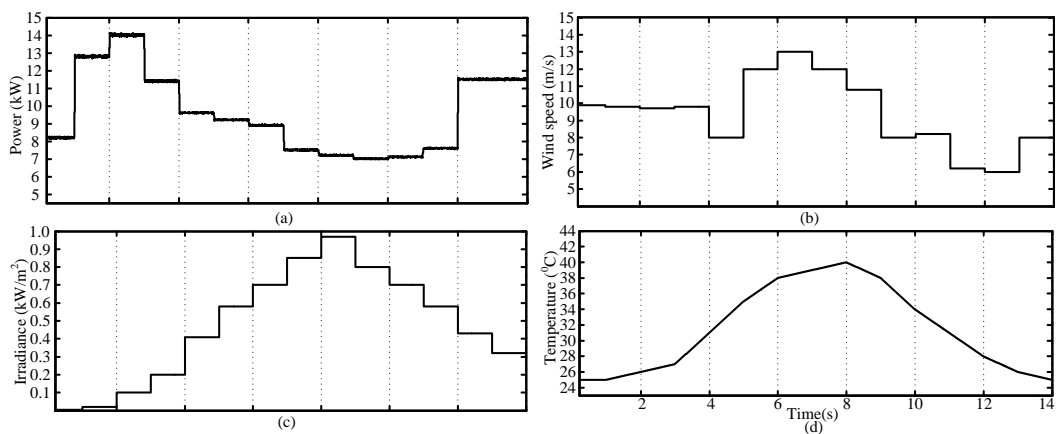

Figure 15: Powers.
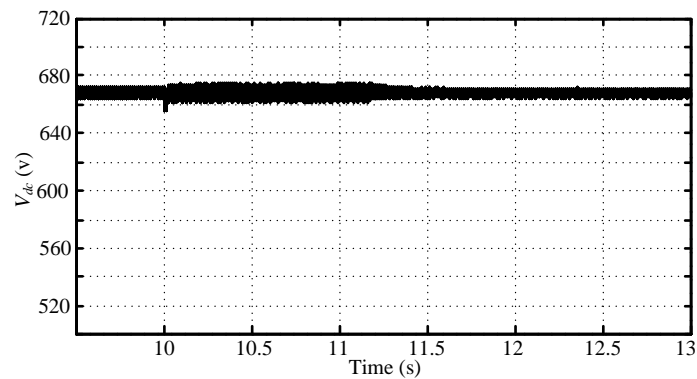
Figure 16: Voltage.

D.   Case-4: Operation during meteorological changes.

Meteorological variations in weather conditions are taken into account to evaluate the efficiency of the microgrid. The analysis focuses on the fluctuations in load, temperature, speed, and irradiances, as shown in Figure 17. The different power components used in this investigation are shown in Figure 18. To keep the load and generation in balance, the BSS, FC, and ES work together. The exact reaction of the RMS line voltage at the PCC is shown in Figure 19. Although the AC RMS voltage at PCC may not offer a distinct indication, Figure 20 and Figure 21 provide a comprehensive breakdown of the instantaneous line voltage and currents, respectively.

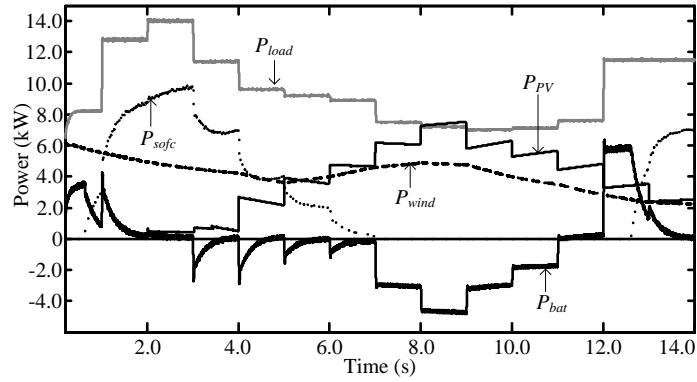**Figure 17: Changes of (a) load, (b) speed, (c) irradiance (d) temperature.**
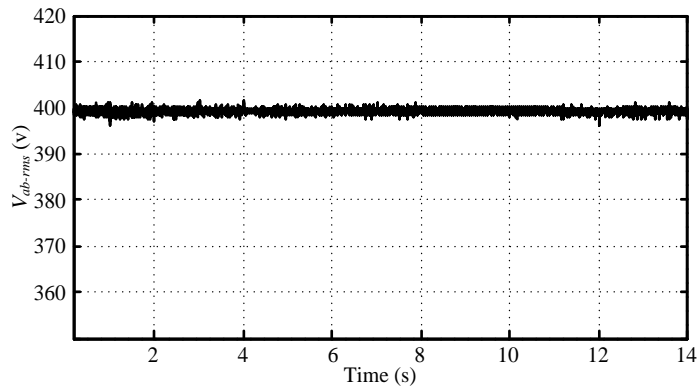
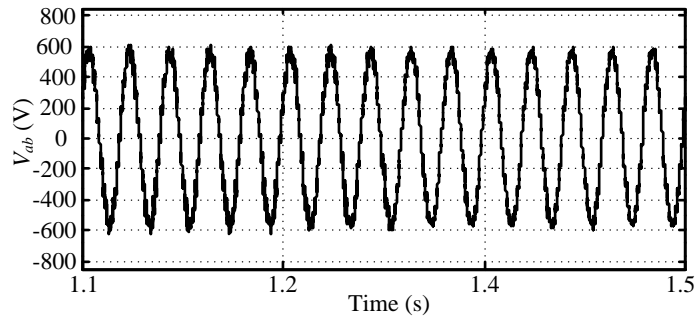**Figure 18: Powers.**

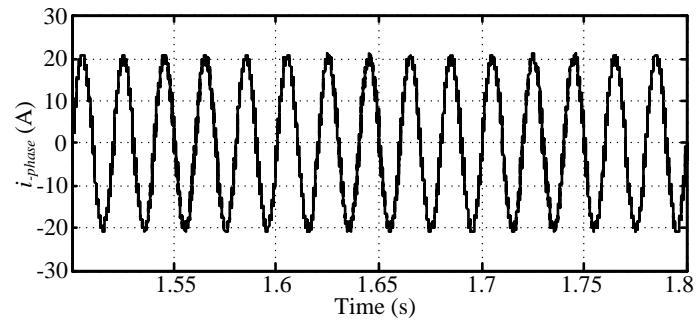**Figure 19: Voltage.**

Figure 20: Voltage.

Figure 21: Currents.

E.   Case-5: Results with various types of loads

The different categories of loads, including constant current, constant power, and constant impedance, can be found in reference [19]. At first, it was thought that the PCC (Point of Common Coupling) was where the resistive load and the constant power load were linked. Below are the parameters for the 5 hp induction motor (IM) that makes up the continuous power load:

Resistances of: Stator = 1.125Ω, Rotor = 1.079Ω.

Stator and rotor inductances = 0.006174H.

Figures 22 and 23 display the powers and dc-link voltages for the IM, which is experiencing a load torque of 40.0Nm. Similarly, figures 24 and 25 indicate the powers and voltage at the DC-link for a constant impedance load (R-L-C series load) following a comparable procedure.
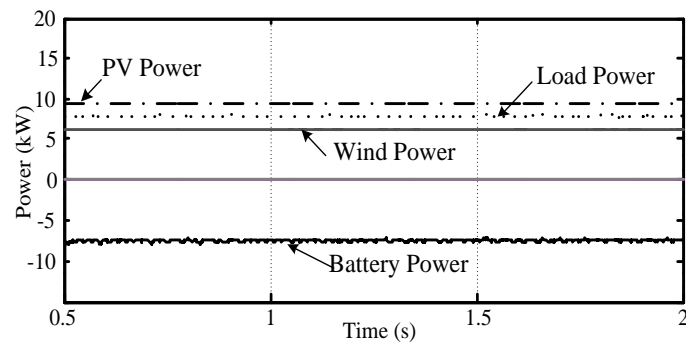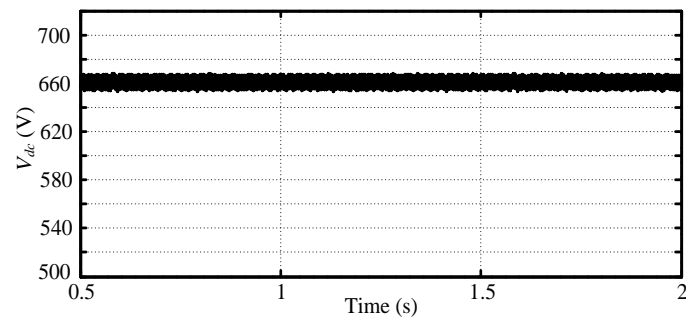

Figure 22: Powers.

Figure 23: V_{dc} **for constant power load.**
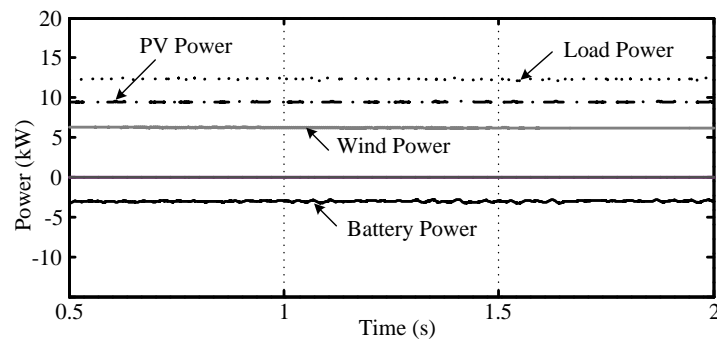

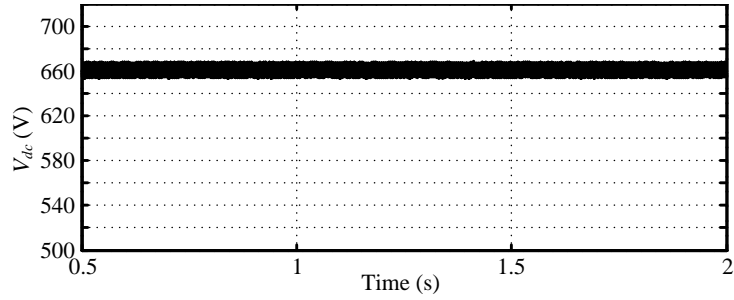**Figure 24: Powers under the operation of constant impedance load.**

Figure 25: V_{dc} at DC-link.

The microgrid is undergoing testing with a constant current load, specifically speed controlled DC drives operated at the PCC. As shown in Figure 26(a), the load torque is kept constant at 15.0 Nm throughout the experiment, with the speed varying between 100 and 200 rpm. As shown in Figure 26(b), the armature voltage is adjusted by changing a chopper's duty cycle to control the motor speed. Figure 27 depicts the different powers involved in this scenario, while Figure 28 shows the equivalent DC-link voltage.
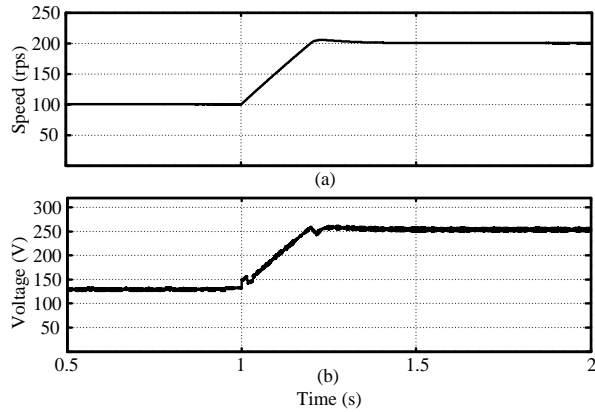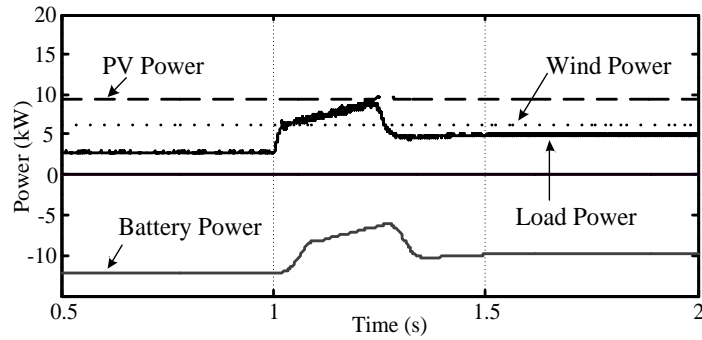

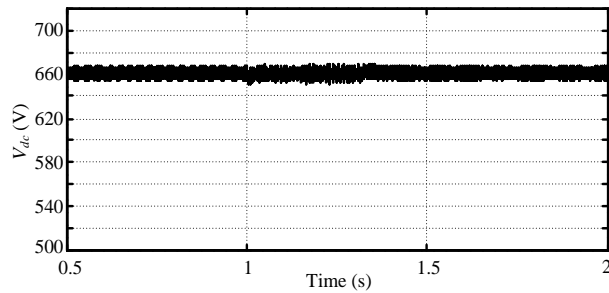**Figure 26: (a) speed, (b) voltage.**

Figure 27: Powers.

Figure 28: V_{dc}.

F.   Case-6: Performance with WOA

The GA, GWO, PSO, and WOA algorithms are utilized for the purpose of minimizing the cost function and optimizing hydrogen production in a given microgrid. By employing these optimization techniques, the cost function can be minimized in order to obtain the most optimal solution [21]. The replies are shown in a system per unit, with the remaining values being relative to the greatest value, which is normalized to '1' per unit. Figure 29 shows the replies for the various categories. The chart illustrates that the WOA algorithm is more efficient in lowering microgrid costs than GA, GWO, and PSO, with GA having the highest cost (shown as '1' per unit). Additionally, the suggested WOA algorithm increases hydrogen generation, which facilitates prompt decision-making amid diverse transitions. Normalized to '1' per unit, WOA achieves the maximum productivity, while the other optimization methods get relative values. Lastly, an illustration of the time response of the different optimization techniques shows that WOA requires much less time to reach appropriate judgments due to its quick tracking capabilities in locating the cost function's lowest point.
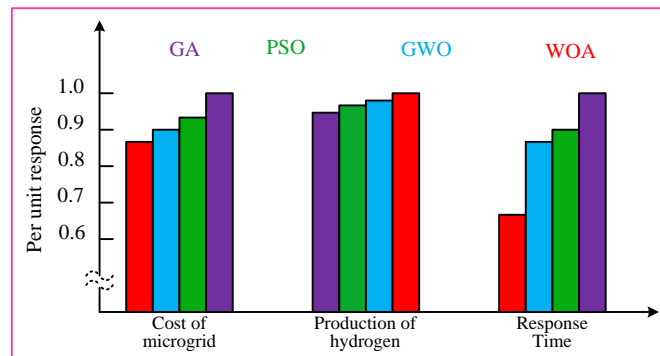
Fig. 29: Comparisons of optimization methods.

V.   CONCLUSIONS

An effective EMS is introduced for microgrids based on RESs, utilizing coordinated control to enhance power quality and hydrogen generation efficiency while minimizing operational costs. The suggested control techniques are intended to guarantee balanced voltages at the PCC and lessen the effects of second harmonic distortions under unbalanced loads. The results of the simulation show that even in the face of variations in load, wind speed, and solar irradiation, the suggested controllers are able to manage load voltages with effectiveness. To attain cost efficiency, WOA is used to optimize the microgrid's cost function. The research emphasizes the significance of WOA by comparing the performance of microgrid optimization strategies. The findings are shown by analyzing many load models, such as constant power, constant impedance, and constant current loads. Simulink and RTDS are used to evaluate and present the results in various circumstances.

CONFLICT OF INTERESTS

Lack of Personal Interest for the publication of this research works.

REFERENCES

[1]   C. N. Bhende, S. Mishra and S. G. Malla, "Permanent Magnet Synchronous Generator-Based Standalone Wind Energy Supply System," IEEE Transactions on Sustainable Energy, vol. 2, no. 4, pp. 361-373, Oct. 2011, doi: 10.1109/TSTE.2011.2159253.

[2]   H. U. R. Habib et al., "Optimal Planning and EMS Design of PV Based Standalone Rural Microgrids," in IEEE Access, vol. 9, pp. 32908-32930, 2021, doi: 10.1109/ACCESS.2021.3060031.

[3]   M. H. Saeed, W. Fangzong, B. A. Kalwar and S. Iqbal, "A Review on Microgrids' Challenges & Perspectives," in IEEE Access, vol. 9, pp. 166502-166517, 2021, doi: 10.1109/ACCESS.2021.3135083.

[4]   D. Steward, G. Saur, M. Penev and T. Ramsden, "Lifecycle Cost Analysis of Hydrogen Versus Other Technologies for Electrical Energy Storage", *Technical Report*, *National Renewable Energy Laboratory (NREL)*, Nov. 2009.

[5]   W. Jiang and B. Fahimi, "Active Current Sharing and Source Management in Fuel Cell–Battery Hybrid Power System", *IEEE Transactions on Industrial Electronics*, Vol. 57, No. 2, pp. 752-761, Feb. 2010.

[6]   B. M. Nguyen, T. Tran, T. Nguyen and G. Nguyen, "Hybridization of Galactic Swarm and Evolution Whale Optimization for Global Search Problem," in IEEE Access, vol. 8, pp. 74991-75010, 2020, doi: 10.1109/ACCESS.2020.2988717.

[7]   S. G. Malla et al., "Whale Optimization Algorithm for PV Based Water Pumping System Driven by BLDC Motor Using Sliding Mode Controller," in IEEE Journal of Emerging and Selected Topics in Power Electronics, vol. 10, no. 4, pp. 4832-4844, Aug. 2022, doi: 10.1109/JESTPE.2022.3150008.

[8]   C. Wang and M. H. Nehrir, "Power Management of a Stand-Alone Wind/Photovoltaic/Fuel Cell Energy System", *IEEE Transactions on Energy Conversion*, Vol. 23, No. 3, pp. 957-967, Sep. 2008.

[9]   Kodjo Agbossou, Mohanlal Kolhe, Jean Hamelin and Tapan K. Bose, "Performance of a Stand-Alone Renewable Energy System Based on Energy Storage as Hydrogen", *IEEE Transactions on Energy Conversion*, Vol. 19, No. 3, pp. 633-640, Sept. 2004.

[10] H. Caliskan, I. Dincer and A. Hepbasli, "Energy, Exergy and Sustainability Analyses of Hybrid Renewable Energy Based Hydrogen and Electricity Production and Storage Systems: Modeling and Case Study", *Applied Thermal Engineering*, In press (available online 21 April 2012).

[11] W. Gao, V. Zheglov, G. Wang and S. M. Mahajan, "PV - Wind - Fuel Cell - Electrolyzer Micro-grid Modeling and Control in Real Time Digital Simulator", *International Conference on Clean Electrical Power*, USA, pp. 29-34, June 2009.

[12] D. Ipsakis, S. Voutetakis, P. Seferlis, F. Stergiopoulos and C. Elmasides, ,"Power Management Strategies for a Stand-Alone Power System using Renewable Energy Sources and Hydrogen Storage", *International Journal of Hydrogen Energy*, Vol. 34, No. 16, pp. 7081-7095, Aug. 2009.

[13] O. Erdinc and M. Uzunoglu, "The Importance of Detailed Data Utilization on the Performance Evaluation of a Grid-Independent Hybrid Renewable Energy System", *International Journal of Hydrogen Energy*, Vol. 36, No. 20, pp. 12664-12677, Oct. 2011.

[14] E. Dursun and O. Kilic, "Comparative Evaluation of Different Power Management Strategies of a Stand-Alone PV/Wind/PEMFC Hybrid Power System", *International Journal of Electrical Power and Energy Systems*, Vol. 34, No. 1, pp. 81–89, Jan. 2012.

[15] P. Enjeti and S. Kim, "A new DC-side active filter for inverter power supplies compensates for unbalanced and nonlinear loads," *Proceedings of IEEE Industry Applications Society Annual Meeting*, Vol. 1, pp. 1023-1031, 1991.

[16] Z. W. Geem, "Size Optimization for a Hybrid Photovoltaic–Wind Energy System", *International Journal of Electrical Power and Energy Systems*, Vol. 42, No. 1, pp. 448-451, Nov. 2012.

[17] Phommixay, Sengthavy, et al. "Review on the cost optimization of microgrids via particle swarm optimization", *International Journal of Energy and Environmental Engineering*, vol. 11, no. 1, Mar. 2020.

[18] R. Robichaud, G. Mosey and D. Olis, "Renewable Energy Optimization Report for Naval Station Newport", *Technical Report NREL*, Feb. 2012.

[19] B. K. Mathur, "The Modeling of Load Characteristics Representation in System Studies", *IEEE Transactions on Industry Applications*, Vol. IA-20, No. 1, pp. 167-172, Jan. 1984.

[20] Kandi Bhanu Prakash, "Modeling of DC to DC Converter for Renewable Energy Sources", International Journal of New Technologies in Science and Engineering (IJNTSE), Vol. 9, Issue. 1, pp. 6-10, Jan. 2023.

[21] M. W. Alzahlan, F. S. El-Faouri, M. G. Batarseh, A. Mohammad and M. E. Za'ter, "Particle Swarm Optimization of a Microgrid's Cost Function Involving Distributed Generation and Highly Fluctuating Load," IEEE Jordan International Joint Conference on Electrical Engineering and Information Technology (JEEIT), 2019, pp. 319-324, doi: 10.1109/JEEIT.2019.8717494.